



Instrument observation strategy for a new generation of three-axis-stabilized geostationary meteorological satellites from China

Jian Shang¹, Lei Yang¹, Pan Huang², Huizhi Yang², Chengbao Liu¹, Jing Wang¹, Lei Zhao¹, Shengxiong Zhou³, Xiaodong Chen², and Zhiqing Zhang¹

¹National Satellite Meteorological Center, China Meteorological Administration, Beijing, 100081, China

²Beijing Institute of Electrical and Mechanical Engineering, Beijing, 100074, China

³Southwest Electronics and Telecommunication Technology Research Institute, Chengdu, 610000, China

Correspondence: Lei Yang (yangl@cma.gov.cn) and Zhiqing Zhang (zqzhang@cma.gov.cn)

Received: 15 July 2018 – Discussion started: 13 March 2019

Revised: 13 June 2019 – Accepted: 26 June 2019 – Published: 18 July 2019

Abstract. The Fengyun-4 (FY-4) satellite series is a new generation of geostationary meteorological satellites from China. The newly adopted three-axis-stabilized attitude-control platform can increase observation efficiency and flexibility while bringing great challenges for image navigation as well as integrated observation mode design. Considering the requirements of earth observation, navigation and calibration as well as observation flexibility, instrument observation strategies are proposed. These include the earth, the moon, stars, cold space, blackbody and diffuser observations on which the instruments' in-orbit daily observations must be based. The most complicated part is the star observation strategy, while navigation precision is dependent on in-orbit star observations. A flexible, effective, stable and automatic star observation strategy directly influences star data acquisition and navigation precision. According to the requirement of navigation, two specific star observation strategies for the two main instruments on board FY-4A were proposed to be used in the operational ground system. The strategies have been successfully used in FY-4A in-orbit tests for more than a year. Both the simulation results and in-orbit application results are given, including instrument observation strategies, star observation strategies and moon observation tasks, to demonstrate the validity of the proposed observation strategies, which lay important foundations for the instruments' daily operation.

1 Introduction

The Fengyun (FY) series of meteorological satellites, operated by the National Satellite Meteorological Center, China Meteorological Administration, has played an important role in meteorological forecasting, cloud detection and precipitation measurement. The Fengyun-4 (FY-4) satellite series is China's new generation of geostationary meteorological satellites, which are three-axis stabilized instead of spin stabilized as in Fengyun-2 (FY-2) satellites. The three-axis-stabilized attitude-control mode can effectively increase observation efficiency and flexibility (NOAA and NASA, 2005) as the satellite can make observations at any time, while the spin-stabilized satellite can only observe the earth when it sweeps across it. The full-disk observation time is shorted from 30 to 15 min. Also, many different kinds of observation tasks can be designed for FY-4, which is impossible for FY-2. However, it brings great challenges for image navigation and registration (INR) compared to spin-stabilized satellites, which can satisfy the navigation requirement just by using edge detection of the earth's disk, making use of the time series dataset of the satellite orientation with respect to the center line of the earth's disk that contains information on the attitude and the misalignment (Lu et al., 2008). Image navigation is an essential and fundamental component in the data processing of geostationary meteorological satellites. The purpose of image navigation is to acquire each image pixel's latitude, longitude, height and other auxiliary angle information. The uncertainty in the instrument's line of sight is the

main error source for navigation (Yang and Shang, 2011). The thermal source in space changes enormously, which can lead to thermal deformation of more than a thousand microradians. The main forms of thermal conduction are radiation and conduction, and the thermal environment of space orbit is very abominable because it lacks important convection. A spin-stabilized satellite tends to equalize the thermal variation seen by the instrument over the day, whereas the thermal gradients across the three-axis-stabilized platform are more extreme (Li et al., 2007; Harris and Just, 2010), which can exceed hundreds of microradians per hour. This can introduce thermal distortions in the platform structure causing changes in the instrument-to-platform alignment. The INR challenge of three-axis-stabilized geostationary satellites mainly comes from thermal elastic deformation from the solar source, launch vibration, orbit measurement error and attitude measurement error. The misalignment caused by thermal elastic deformation, which cannot be measured directly, is the most difficult element to model (Shang et al., 2017). The misalignment must be calculated and forecasted accurately in the ground system. With uploaded coefficients, compensation could be accomplished by the onboard system. Thus, navigation is fulfilled by a complicated satellite–earth integrated operation (Li and Dong, 2008; DOC et al., 2016, 2017).

Due to the complication of the navigation of three-axis-stabilized geostationary satellites, more precise navigation methods shall be considered. Star sensing using the instruments on board the satellite sheds new light on image navigation of three-axis-stabilized geostationary satellites. It has many advantages versus landmark navigation, which has been used widely in remote sensing image processing. Stars are ideal point sources and their position on the celestial sphere can be determined precisely. Stars can be observed in both day and night and can obtain the line of sight directly (Li et al., 2007). Before star navigation, there is much work to be carried out, among which establishing star observation strategies for different instruments is fundamental and difficult. The strategies, which are constrained by a lot of conditions, need to select the most proper stars from a number of stars observed in the instrument's field of view, and within the given observation time determined by instrument time schedule. Then, based on star observation strategies, considering the integrated requirements of navigation, calibration and earth observation, instrument observation strategies should be developed to guide the instruments to automatically carry out every in-orbit observation.

This paper is a foundation for FY-4 image navigation work concerning task planning. It focuses on the instrument observation strategies as well as flexible and automatic star observation strategies for FY-4 main instruments. Simulations are carried out to give long-term analysis. The first satellite of the FY-4 satellite series, FY-4A, was launched on 11 December 2016. In-orbit test results are obtained and used to demon-

Table 1. Main parameters of AGRI.

Index	Parameter
Bands	14
Spatial resolution	visible: 0.5–1 km near-infrared: 2 km infrared: 4 km
Temporal resolution	15 min/full disk
Field of observation	21° N–S × 23° E–W, with a regional observation ability
Star sensing ability	6 Mv (visual magnitude)
Navigation accuracy	1 infrared pixel
Calibration accuracy	0.5–1 K

strate the effectiveness of the strategies, which pave the way for high-accuracy navigation of FY-4A.

2 Instrument observation strategies

FY-4 instruments' in-orbit observations are more flexible than that of FY-2 satellite as FY-4 satellites use a three-axis-stabilized platform instead of a spin-stabilized platform, and are thus more complicated. Towards the two main instruments aboard FY-4A, the Advanced Geosynchronous Radiation Imager (AGRI) and Geosynchronous Interferometric Infrared Sounder (GIIRS), instrument observation strategies are designed to figure out their in-orbit observation task modes, making full use of the observation time and flexibility.

2.1 AGRI observation strategy

The geostationary imager is the most effective instrument on board the geostationary satellites all over the world. AGRI is the core instrument of FY-4A satellite, which aims to carry out high temporal and spatial resolution imaging of the atmosphere, cloud, land and ocean with over 14 spectral bands in the visible (VIS), near-infrared (NIR) and infrared (IR) spectral regions, providing important information for weather analysis and forecasting, climate research, environment and disaster monitoring (Zhang et al., 2016; Dong, 2016). Main parameters of AGRI are shown in Table 1, and information on its 14 bands is summarized in Table 2.

AGRI's main objective is to carry out imaging of earth's full disk. Besides this, higher temporal resolution imaging of China and certain interesting regions is very important for regional weather forecasting and disaster monitoring. Hemispheric observation should also be arranged as required. From a navigation and registration perspective, periodical star observations, landmark observations and the moon observations are obligatory. From a calibration perspective, blackbody, cold space, diffuser and moon must be observed. In all, 17 observation modes are designed for AGRI as listed in Table 3, considering high-sensitivity scan as well as nor-

Table 2. Spectral configuration of AGRI.

No.	Central band(μm)	Spectral band(μm)	Main applications
1	0.47	0.45–0.49	aerosol, color image synthesis
2	0.65	0.55–0.75	vegetation, star sensing
3	0.825	0.75–0.90	vegetation, aerosol
4	1.375	1.36–1.39	cirrus
5	1.61	1.58–1.64	cloud, fire
6	2.225	2.10–2.35	cirrus, aerosol
7	3.375	3.50–4.00	cloud, fire/land surface
8	6.25	5.80–6.70	upper-level water vapor
9	6.95	6.75–7.15	mid-level water vapor
10	7.42	7.24–7.60	low-level water vapor
11	8.70	8.40–9.00	integrated water vapor, cloud
12	10.80	10.30–11.30	cloud, temperature
13	12.00	11.50–12.50	cloud, integrated water vapor, temperature
14	13.50	13.20–13.80	cloud, water vapor

Table 3. Observation modes of AGRI.

No.	Observation mode	Observation type
1	Full disk	Normal scan/high-sensitivity scan
2	Northern Hemisphere	Normal scan/high-sensitivity scan
3	Southern Hemisphere	Normal scan/high-sensitivity scan
4	China	Normal scan/high-sensitivity scan
5	Regional	Normal scan/high-sensitivity scan
6	Moon	Normal scan/high-sensitivity scan
7	Landmark	Normal scan/high-sensitivity scan
8	Star	Dwell
9	Blackbody	Dwell
10	Diffuser	Dwell

mal scan modes with regard to earth observation (Shang et al., 2018). Infrared background observations, which are also needed to provide background data for infrared band data processing, are, in essence, cold-space observations at different positions and thus are not listed in Table 3. Nowadays full-disk observations and observations of China are chosen as the main earth observation modes. In every time block, one full-disk task or three Chinese region tasks, one infrared background task, one blackbody task and one star observation task are arranged in the time schedule, which is used by the whole ground system to operate on schedule. The star observation strategy is the most complicated part of the instrument observation strategy, which will be proposed below in detail. Landmark and cold-space observations are contained in the full-disk task automatically. This guarantees routine earth observation along with fundamental requirements of navigation and calibration. The diffuser task will be inserted into the time schedule when the computed solar declination angle is suitable.

The positions of the sun and the moon in the International Celestial Reference System at any time are obtained from

Table 4. Main parameters of GIIRS.

Index	Parameter
Spectral parameter	longwave IR: 700–1130 cm^{-1} medium shortwave IR: 1650–2250 cm^{-1} visible: 0.55–0.75 μm
Spectral resolution	longwave IR: 0.8 cm^{-1} medium shortwave IR: 1.6 cm^{-1}
Spatial resolution	visible: 2 km infrared: 16 km
Temporal resolution	35 min (1000 km \times 1000 km) 67 min (5000 km \times 5000 km)
Field of observation	22.2° circle, with a regional observation ability
Star sensing ability	6.5 Mv (visual magnitude)
Navigation accuracy	1 infrared pixel
Radiation calibration accuracy	1.5 K
Spectrum calibration accuracy	10 ppm

high-precision DE412 data (Development Ephemeris 412) released by NASA JPL (National Aeronautics and Space Administration, Jet Propulsion Laboratory), recommended by the IAU (International Astronomical Union). The positions are transformed into the geocentric celestial reference system and then inertial coordinate system. If the sun is forecasted to appear in the vicinity of AGRI's field of view, its influence on star sensing, cold-space observation, earth observation or the motion track of scanning mirrors must be considered in order to ensure the observation validity as well as the safety of the instrument. Moon task will be inserted automatically into the time schedule when the moon is forecasted to appear in AGRI's field of view. The instrument's pointing angles of the moon are computed finally in the instrument coordinate system, which will be written into the observation instruction parameter file and uploaded to the satellite.

2.2 GIIRS observation strategy

GIIRS is another important instrument on board FY-4A. Its main objective is to detect atmospheric temperature, moisture and trace-gas content precisely, providing input data for numerical weather forecasts, disastrous weather monitoring and atmospheric chemical composition detection. It has visible, medium shortwave and longwave IR bands. Main parameters of GIIRS are shown in Table 4 (Zhang et al., 2016; Dong, 2016).

As mentioned above, GIIRS's main detection mode is dwell detection of the atmosphere. From a navigation perspective, periodical star observation and landmark observation are obligatory. A unique ground-based laser system is proposed to assist GIIRS's navigation. From a calibration perspective, blackbody, cold space and the moon must be observed. In all, seven observation modes are designed for GI-

Table 5. Observation modes of GIIRS.

No.	Observation mode	Observation type
1	Region	Step dwell
2	Moon	Dwell
3	Landmark	Step dwell
4	Star	Dwell
5	Laser	Step dwell
6	Blackbody	Dwell
7	Cold space	Dwell

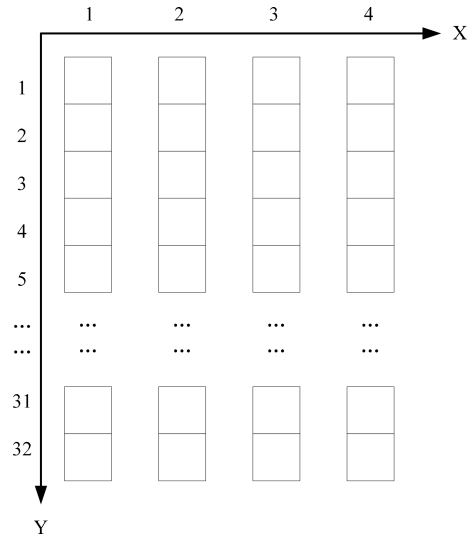
IRS as listed in Table 5. In every time block, one region task, one blackbody task, one cold-space task and one star task are arranged in the time schedule, which guarantees routine earth observation along with fundamental requirements of navigation and calibration. The landmark task is arranged periodically to estimate navigation precision, interrupting routine region task, and thus can not be carried out frequently. In addition, the moon task will be automatically inserted when the moon is forecasted to appear in GIIRS's field of view, which is a little different from AGRI and should be forecasted. Also, the sun must be forecasted in advance to ensure the observation validity as well as the safety of the instrument.

3 Star observation strategies

The two main instruments aboard FY-4A are designed with the ability to sense stars of magnitudes at least lower than 6.0 to help to achieve high accuracy of image navigation in the three-axis-stabilized attitude-control platform. The ground system first forecasts all the stars that will appear in the instrument's field of view at the given time. Then proper stars (optimum stars needed for satellite navigation) are chosen according to a complicated star observation strategy, exclusively developed for the instrument. The star observation instructions are then automatically generated and uploaded to the satellite. For star sensing, the instrument is commanded to dwell at angles determined by the ground system for a given star crossing. The instrument's inertial viewing angles then drift at earth's rotation rate in a roughly westerly direction as the spacecraft's attitude control continuously aligns the instrument boresight with the earth (Gibbs et al., 2008).

3.1 AGRI star observation strategy

The 1-pixel accuracy of navigation of AGRI is one of the most difficult tasks in satellite–earth integrated operation. Thus, star navigation is indispensable. AGRI has 14 observation bands, the second (0.55–0.75 μm) of which is designed to sense stars of magnitudes higher than 6.0, as shown in Table 2. The detector size is 32 (north–south direction) by 4 (west–east direction) pixels, with a gap between adjacent columns, which is shown in Fig. 1. This must be considered in developing AGRI's star observation strategy to guide its

**Figure 1.** Detector array diagram of AGRI.

in-orbit daily star sensing. Another characteristic of AGRI is its small detector size, which means that for most of the time only one star can be observed. This directly influences the minimal distance between the candidate star and another star.

Star observation strategy of AGRI includes several aspects. Firstly, the frequency of star sensing must be determined, which is mainly determined by the changing regularity of thermal elastic deformation of the satellite platform as well as the instrument, while balancing among different observation tasks. Secondly, the requirements of star centroid extraction must be considered. Thirdly, the requirements to ensure the accuracy of thermal elastic deformation calculation, which is the key issue in image navigation of three-axis-stabilized geostationary satellites, must be considered. The criteria for choosing optimal stars for AGRI are proposed as follows.

1. The main task of AGRI is to carry out earth observation. Star sensing, as an indispensable part of image navigation, should have priority to be arranged periodically besides the earth observation tasks.
2. The gap between adjacent columns is a big disadvantage to star centroid extraction. Thus, dwell observation mode is recommended for star sensing, waiting for the star to cross the whole focal plane, aiming at obtaining star observation data of relatively long time series. This can effectively improve the accuracy of star centroid extraction (Zhang et al., 2018).
3. Considering AGRI's angular resolution, the candidate stars should be separated from each other.

4. The star with lower magnitude should be considered with priority, which is advantageous for star centroid extraction and thus navigation.
5. The magnitude of the target star must be lower than AGRI's observation ability. Meanwhile, it should be higher than the magnitude threshold that may make the image saturated, which will affect normal star centroid extraction.
6. The target star should always be within AGRI's field of view, both at the start and at the end of the observation.
7. The target star should not be shaded by the earth's atmosphere, the sun, the moon, etc.
8. During the observation, the target star must not be shaded by the earth itself.
9. The observation of the target star should not be affected by stars that subsequently entered into the field of view or newly traced out of the earth.
10. Exclude variable stars (variable brightness magnitude) that may have disadvantageous effects on star centroid extraction.
11. Double stars should be selected carefully, balancing the number of proper stars against the effect on star centroid extraction.
12. Finally, and most importantly, the distribution of candidate stars should be strictly constrained to ensure the accuracy of thermal elastic deformation parameter calculation.

The known parameters mainly include AGRI's field of view, angular resolution, the detector size, the given time and time limit of star sensing. A variety of thresholds need to be calculated using these parameters, including minimum resolution threshold, minimum magnitude threshold, maximum magnitude threshold, sun/moon/earth effect threshold, moving threshold, variable star threshold, double star threshold, distribution threshold, etc.

The most important distribution threshold should be determined on the basis of angle distance of two stars. The method to compute angle distance from instrument pointing angles is derived as follows. A plane coordinate system is established in Fig. 2. The coordinate origin is located as the center of the earth. The positive directions of the X axis and Y axis are west and north, respectively. Points S and O denote the satellite and the earth center, respectively. *a* and *b* denote two stars, whose viewing vectors intersect with plane XOY at point A and B. A_X , A_Y , B_X and B_Y are the projection points of the vectors on X and Y axes, respectively. The scan angles in east–west direction and step angles in north–south direction of observing stars *a* and *b* are α_A , β_A , α_B and β_B , respectively.

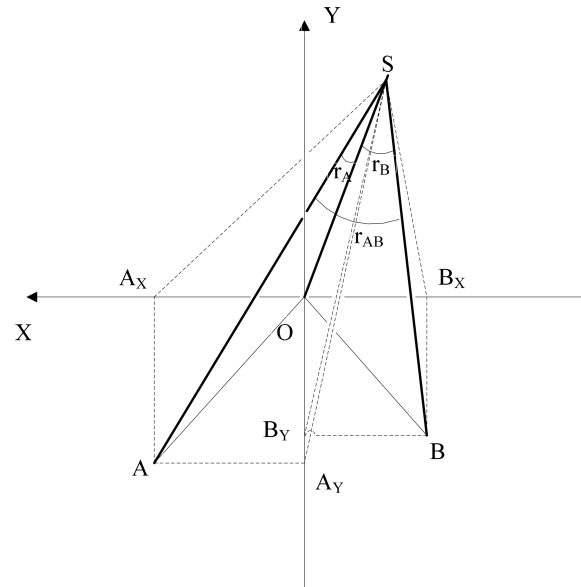


Figure 2. Coordinate system established for computing angle distance.

Angle γ_A and γ_B between stars *a* and *b* are computed as in Eqs. (1) and (2):

$$\tan \gamma_A = \frac{OA}{OS} = \frac{\sqrt{OA_X^2 + OA_Y^2}}{OS}, \tag{1}$$

$$\tan \gamma_B = \frac{OB}{OS} = \frac{\sqrt{OB_X^2 + OB_Y^2}}{OS}, \tag{2}$$

where *OS* is the distance from the satellite to the earth center. From Eqs. (3) and (4), angles γ_A and γ_B can be obtained using Eqs. (5) and (6):

$$\tan \alpha_A = \frac{OA_X}{OS}, \quad \tan \beta_A = \frac{OA_Y}{OS}; \tag{3}$$

$$\tan \alpha_B = \frac{OB_X}{OS}, \quad \tan \beta_B = \frac{OB_Y}{OS}; \tag{4}$$

$$\tan \gamma_A = \sqrt{(\tan \alpha_A)^2 + (\tan \beta_A)^2}; \tag{5}$$

$$\tan \gamma_B = \sqrt{(\tan \alpha_B)^2 + (\tan \beta_B)^2}. \tag{6}$$

Then the angle distance γ_{AB} of stars *a* and *b* is computed using cosine theorem, as in Eq. (7):

$$\cos \gamma_{AB} = \frac{SA^2 + SB^2 - AB^2}{2 \cdot SA \cdot SB}, \tag{7}$$

where

$$\begin{aligned}
 SA &= \frac{OS}{\cos \gamma_A}, \quad SB = \frac{OS}{\cos \gamma_B}; \\
 AB^2 &= OA^2 + OB^2 - 2 \cdot OA \cdot OB \cdot \cos \angle AOB; \\
 OA &= \sqrt{OA_X^2 + OA_Y^2}, \quad OB = \sqrt{OB_X^2 + OB_Y^2}; \\
 \cos \angle AOB &= \frac{\vec{OA} \cdot \vec{OB}}{|\vec{OA}| \cdot |\vec{OB}|} \\
 &= \frac{OA_X \cdot OB_X + OA_Y \cdot OB_Y}{OA \cdot OB}. \quad (8)
 \end{aligned}$$

Based on star observation, star navigation of a three-axis-stabilized geostationary satellite can be realized. The navigation accuracy of AGRI can be estimated as follows. Star navigation accuracy is theoretically determined by the accuracy of attitude measurement, orbit determination, scan mirror pointing control, star centroid extraction and thermal elastic deformation parameter calculation. The navigation accuracy is calculated to be about 14.70 arcsec, corresponding to 2.54 km on the ground observed from geostationary orbit. This navigation accuracy obtained by star observation can satisfy the index of 1 infrared pixel, which corresponds to 4 km on the ground. Thus the great challenge of high-precision navigation brought by three-axis stabilization can be effectively solved.

3.2 GIIRS star observation strategy

Another important instrument aboard FY-4A is GIIRS, which is the first one flying in geostationary orbit and will provide high spectral resolution IR sounding observations over China and adjacent regions (Zhang et al., 2016). The accuracy of GIIRS image navigation is also 1 pixel, and star navigation is introduced into the GIIRS navigation flow. GIIRS is designed deliberately with a visible band (0.55–0.75 μm) to sense stars of magnitudes lower than 6.5. The detector size is 330 (north–south direction) by 256 (west–east direction) and no gap between adjacent columns or rows, which is shown in Fig. 3. Star observation strategy of GIIRS must also be developed, considering both the similarities and differences between AGRI and GIIRS. The similarities include requirements of star centroid extraction and thermal elastic deformation parameter calculation. The main difference comes from the different instantaneous field of view (IFOV) and star sensing ability, which will be analyzed in detail.

1. AGRI's IFOV is 448 μrad (north–south direction) by 98 μrad (west–east direction), while GIIRS's IFOV is 18 480 μrad (north–south direction) by 14 336 μrad (west–east direction). Thus, most of the time AGRI can only observe one star, while GIIRS has the ability to observe two or three stars, sometimes even more. The number of stars which can be observed by AGRI and

Table 6. Statistics of double star data for AGRI.

No.	Right ascension of star 1 (°)	Declination of star 1 (°)	Right ascension of star 2 (°)	Declination of star 2 (°)
1	266.148	2.579	266.142	2.579
2	184.538	−3.954	184.540	−3.949
3	75.136	3.615	75.141	3.616
4	234.667	−8.794	234.667	−8.791
5	70.896	−8.796	70.894	−8.794
6	97.206	−7.034	97.204	−7.033
7	337.207	−0.020	337.209	−0.020
8	133.873	−7.971	133.873	−7.970

GIIRS in the 21° (north–south direction) by 23° (west–east direction) field of view are obtained through simulations, and the statistical results are given in Tables 6 and 7, respectively. Ideal satellite orbit and attitude are used in the coordinate system transformation from the International Celestial Reference Frame (ICRS) to instrument coordinate system. The maximum magnitude analyzed is 7.0. Only a few groups of double stars are found for AGRI, while the percentage of multi-star observations for GIIRS is up to 16 %. This is advantageous for star recognition. And GIIRS's star sensing ability is higher than AGRI, which means there are more stars that can be observed. So multi-star observation is considered with higher priority for GIIRS.

2. In the process of choosing the optimal constellation, many aspects should be considered, including the number of stars in the IFOV, the relative distribution, the minimum distance, the difference of star magnitude, etc. The first one and the second one influence the accuracy of star recognition. The third one and the fourth one influence the accuracy of star centroid extraction.
3. GIIRS detector is so large that the time consumed by the star crossing the whole detector is too long to bear. A small area of less than 10 pixels near the center of the detector is chosen to be used for star sensing in order to save observation time as well as to avoid the effect of distortion at the edge of the detector.

The known parameters mainly include GIIRS's field of view, angular resolution, the detector size, the given time and time limit of star sensing. A variety of thresholds need to be calculated using these parameters, including the thresholds mentioned in AGRI's star observation strategy, as well as the threshold of star number in IFOV, the relative distribution constrain, the minimum distance and the threshold of star magnitude difference within the constellation.

4 Simulation results

The AGRI observation strategy and GIIRS observation strategy are proposed above in detail. In every time block, one

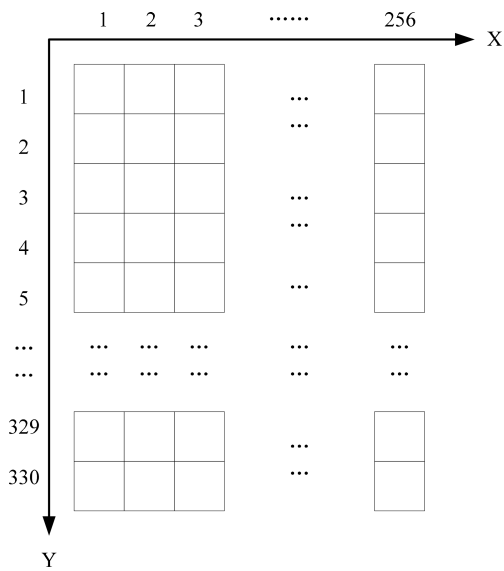


Figure 3. Detector array diagram of GIIRS.

Table 7. Statistics of multi-star data for GIIRS.

No. of stars in IFOV	Occurrence number
9	8
8	18
7	55
6	43
5	74
4	398
3	3421
2	25 844
1	160 302
0	569 397

full-disk task or three Chinese region tasks, one infrared background task, one blackbody task and one star task are arranged for AGRI, while one region task, one blackbody task, one cold-space task and one star task are arranged for GIIRS. The time block is shown in Fig. 4 for clarity. FY-4A’s daily operation is implemented based on these two time blocks.

Before FY-4A was launched, in-depth simulations were carried out to confirm the validity of AGRI and GIIRS star observation strategies, which are the core of instrument observation strategies. An accurate star forecasting module is specially developed for FY-4A. Using coordinate system transformation and time system transformation, the star positions in ICRS are transformed to scanning angles and stepping angles in the instrument coordinate system. Then it is estimated whether the stars can be observed in the instruments’ field of view at the given observation time. Suitable stars with their magnitudes and positions are selected and recorded. Based on these forecasting results, many aspects

Table 8. Star magnitude statistics of AGRI.

Month	3.5–4.5	4.5–5.5	5.5–6.5
January	9.67 %	23.37 %	66.96 %
February	9.75 %	23.65 %	66.61 %
March	9.64 %	23.47 %	66.88 %
April	9.63 %	23.42 %	66.96 %
May	9.67 %	23.52 %	66.81 %
June	9.77 %	23.73 %	66.50 %
July	9.63 %	23.43 %	66.94 %
August	9.77 %	23.72 %	66.51 %
September	9.60 %	23.47 %	66.92 %
October	9.70 %	23.41 %	66.90 %
November	9.66 %	23.58 %	66.76 %
December	9.80 %	23.47 %	66.73 %

Table 9. Star magnitude statistics of GIIRS.

Month	3.5–4.5	4.5–5.5	5.5–6.5	6.5–7.5
January	3.56 %	8.07 %	22.73 %	65.64 %
February	3.53 %	8.05 %	22.27 %	66.15 %
March	3.58 %	7.93 %	22.56 %	65.92 %
April	3.46 %	7.97 %	22.53 %	66.04 %
May	3.69 %	8.00 %	22.31 %	66.00 %
June	3.52 %	8.06 %	22.33 %	66.10 %
July	3.50 %	8.14 %	22.53 %	65.82 %
August	3.49 %	8.09 %	22.47 %	65.95 %
September	3.64 %	8.13 %	22.43 %	65.80 %
October	3.47 %	7.98 %	22.56 %	65.99 %
November	3.61 %	8.21 %	22.51 %	65.68 %
December	3.55 %	7.89 %	22.35 %	66.20 %

of star observation strategies can be analyzed. An important constrain of star observation strategy is star magnitude. The percentages of different star magnitude ranges for AGRI and GIIRS are counted for every month, which are given in Tables 8 and 9, respectively. The larger the magnitude, the more stars there are. But the smaller the magnitude, the higher the accuracy of star centroid extraction. Within the range of 3.5 to 6.5 (7.5), which is determined by AGRI (GIIRS) detecting ability, a few star magnitudes lie in the range of 3.5 to 4.5, which are more likely to be selected in star observation strategy. Moreover, distribution and many thresholds mentioned above must be considered comprehensively.

The stars for the whole year of 2017 that could be observed by the instruments are forecasted. Then optimal stars are selected for AGRI and GIIRS automatically, according to the proposed star observation strategies. In the simulation, both AGRI and GIIRS carry out 35 040 star observation tasks in 2017. Tables 10 and 11 respectively present the statistical number of selected stars for AGRI and GIIRS in every month. As FY-4A flies in a geostationary orbit, the daily star observation situation is similar. For AGRI, the number of selected observable stars for each star measurement lies within

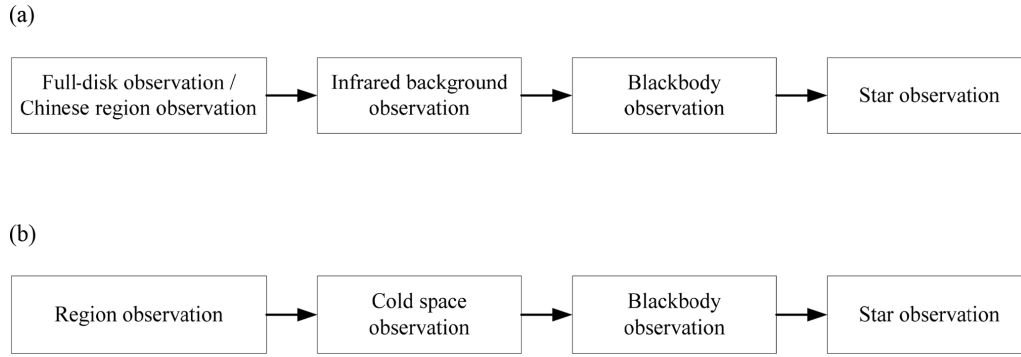


Figure 4. Time blocks for AGRI and GIIRS used in daily operation: (a) AGRI and (b) GIIRS.

Table 10. The number of AGRI selected stars in every month.

Month	Maximum	Minimum	Mean
January	39	6	17.38
February	38	5	17.43
March	38	5	17.37
April	39	6	17.4
May	38	5	17.34
June	38	5	17.39
July	39	6	17.36
August	38	5	17.37
September	39	5	17.37
October	39	6	17.39
November	38	5	17.37
December	38	5	17.38

Table 11. The number of GIIRS selected stars in every month.

Month	Maximum	Minimum	Mean
January	50	7	20.99
February	48	8	20.96
March	51	8	20.98
April	48	8	20.94
May	49	8	20.99
June	50	8	20.96
July	50	7	21.00
August	48	8	20.96
September	51	8	21.00
October	48	8	20.97
November	49	8	20.99
December	50	8	20.97

the range from 5 to 39. For GIIRS, the number lies within the range from 7 to 51. Therefore, it can be concluded that all the cases can ensure adequate observation data needed for thermal elastic deformation parameter calculation.

A specialized software was developed to demonstrate the observable stars, in which all the observable stars as well as finally selected optimal stars can be seen clearly. Figures 5

and 6 give three different examples of AGRI and GIIRS star selection, respectively, in which five stars are set as the goal. The outer frame represents the instruments’ observation range, where the abscissa represents scanning angle and the ordinate represents stepping angle. Figures 5a and 6a show the case of too many stars that can be selected. Figures 5b and 6b show the case of neither too many nor too few stars. Figures 5c and 6c show the case of only a few stars. In each case, five stars are all selected successfully, using the proposed star observation strategies. And the relative distributions, which are one of the most important aspects in thermal elastic deformation parameter calculation, are very reasonable. Figures 5 to 12 are from the interface of FY-4A ground system we constructed.

5 In-orbit application results

Since FY-4A was launched at the end of 2016, the specifically developed instrument observation strategy software has been used in the ground system. On receiving AGRI and GIIRS’s time schedules, the specially developed software firstly forecasts observable stars and selects optimal ones automatically. Then accurate execution times are computed for each star observation task, according to the rules of mirror movement, and star observation instruction parameters are generated. Other tasks, including full disk, regional, blackbody, etc., are separated into the smallest pieces and accurate execution times are computed. Sun avoidance must be carefully considered while designing the mirror movements to protect the instruments. Finally, the complete observation instruction parameters corresponding to the whole time schedule are packed together and uploaded to the satellite. AGRI and GIIRS will carry out in-orbit observations automatically at fixed times according to the instructions. The whole process, including star selection, instruction parameter generation, instruction uploading and in-orbit observation is fully automatic and there is no need for manual intervention under normal circumstances.

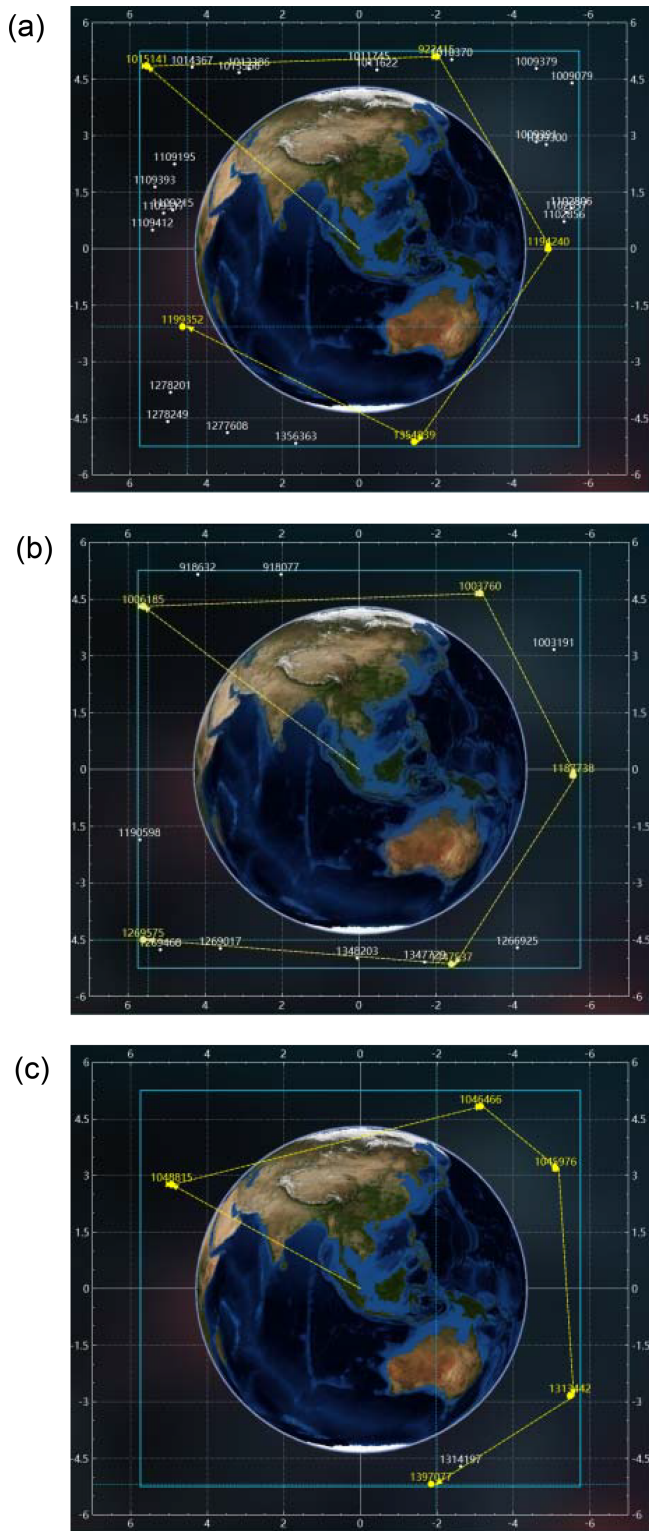


Figure 5. Examples of AGRI star selection results: panel (a) with a lot of stars, (b) with a reasonable number of stars and (c) with a few stars.

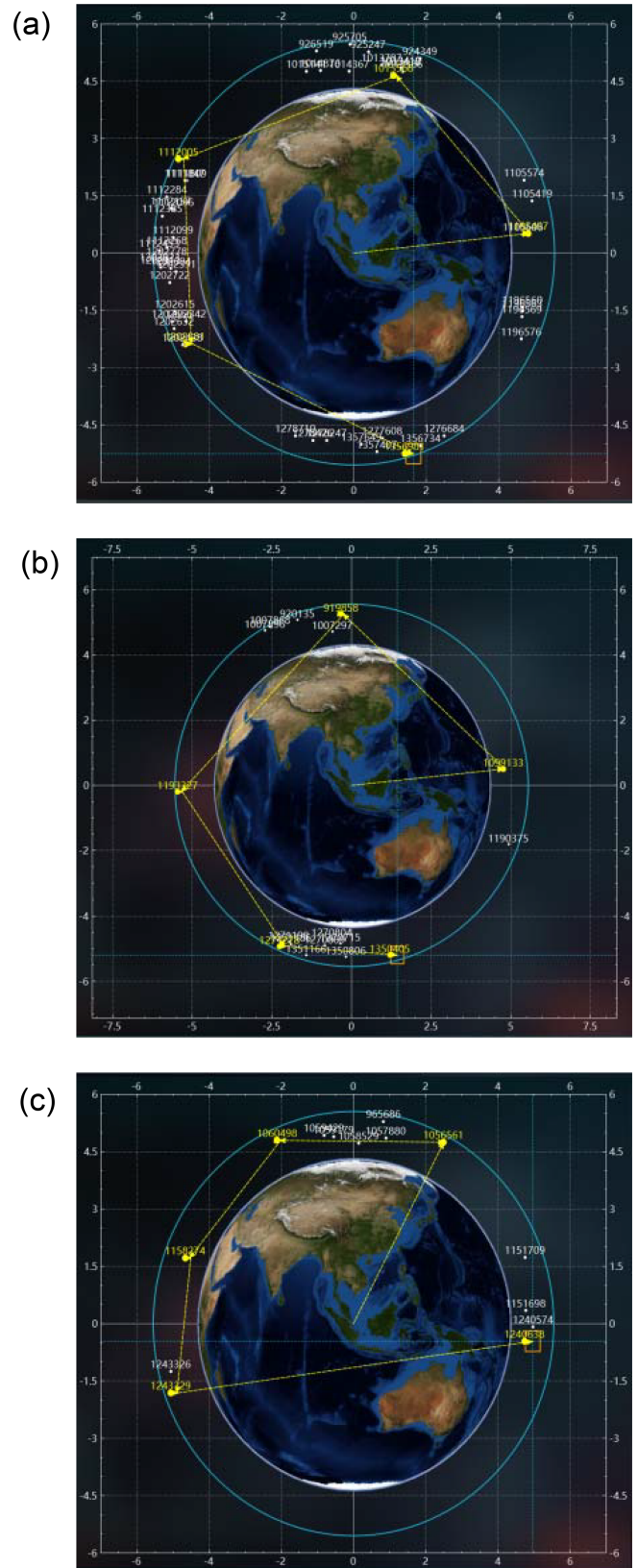


Figure 6. Examples of GIIRS star selection results: panel (a) with a lot of stars, (b) with a reasonable number of stars and (c) with a few stars.

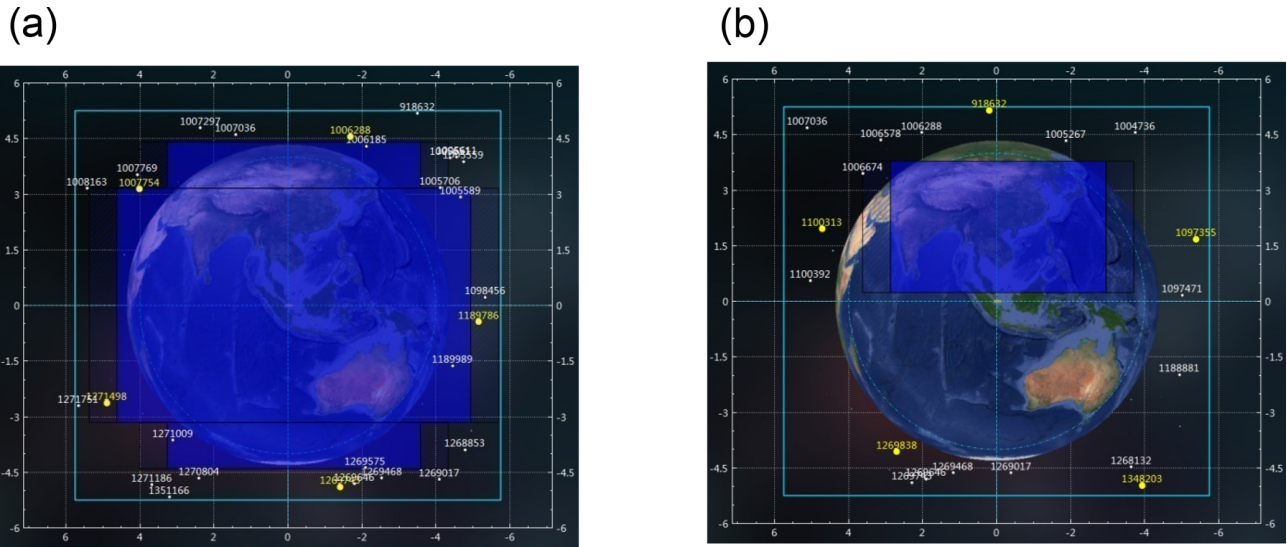


Figure 7. AGRI typical tasks: (a) full-disk observation and (b) Chinese region observation.

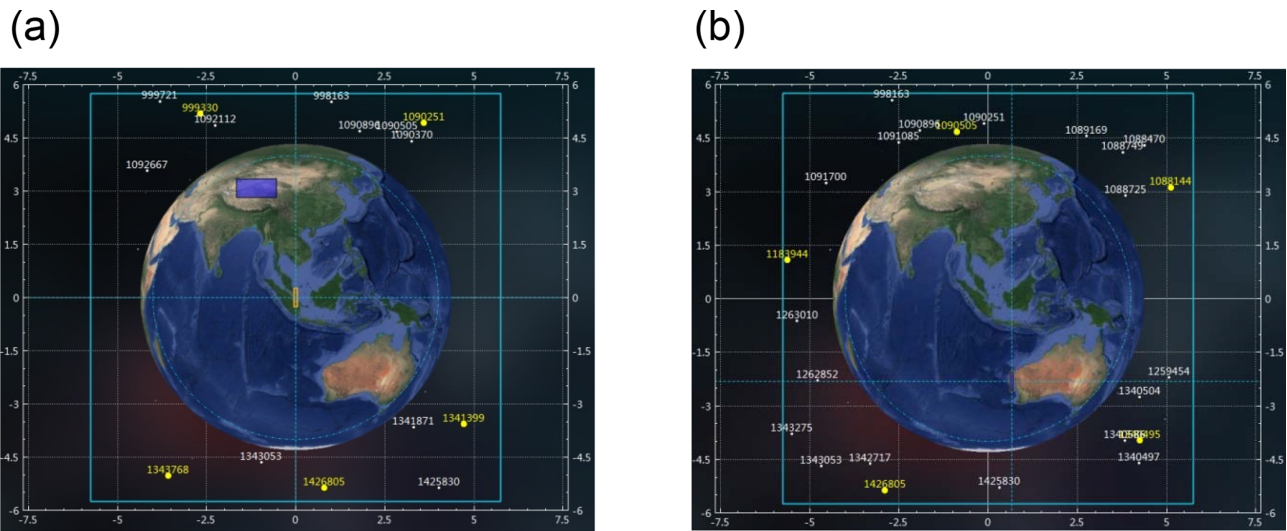


Figure 8. GIIRS typical tasks: (a) regional observation of China and (b) landmark observation of the western coastline of Australia.

From March 2017 to March 2018, the software of the instrument observation strategy has been operating well and generated more than 163 000 tasks and 1 163 000 instructions for AGRI, and more than 169 000 tasks and 1 047 000 instructions for GIIRS. Figures 7 and 8 give typical examples of AGRI and GIIRS tasks. The abscissa represents the instruments' scanning angle and the ordinate represents stepping angle. Plenty of the earth surface, atmosphere and cloud observation data have been provided to users of weather forecasts, climate change, disaster monitoring and environment surveillance.

Actual star selection results of different numbers of stars in the operational ground system are given as follows. Figure 9 demonstrates the case that the sun is not in AGRI's field of

view, when the effect of solar stray light does not need to be considered and the useful field to select stars is relatively large. Figure 10 demonstrates the case that the sun appears in or near AGRI's field of view, when the effect of solar stray light may be obvious and must be considered. Thus the useful field to select stars can be much smaller, and resulting star selection more difficult. In this case, the requirement of a large number of stars cannot be satisfied. Figures 11 and 12 are different cases of GIIRS. The abscissa represents the instruments' scanning angle and the ordinate represents stepping angle.

Using the specifically developed software of the star observation strategy, statistics of star selection tasks of AGRI and GIIRS are given in Tables 12 and 13, respectively. The sta-

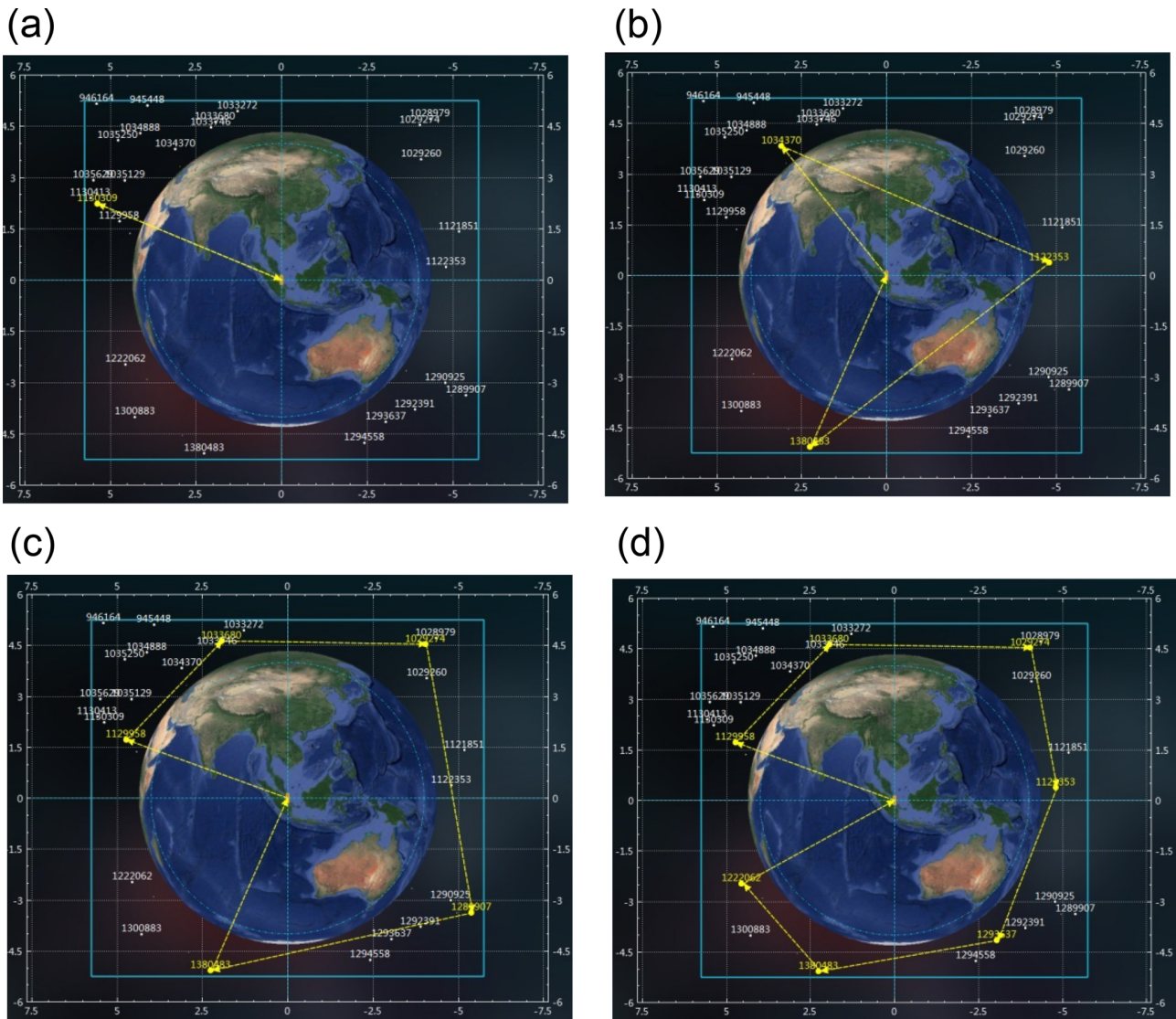


Figure 9. AGRI star selection results – without the sun: (a) the result of choosing one star, (b) the result of choosing three stars, (c) the result of choosing five stars and (d) the result of choosing seven stars.

tistical period is from March 2017 to March 2018. Different situations encountered include changing field of view, forecast period, magnitude range, star number, star constellation constraint and so on. The success rate of software operation is 100 %, validating that the proposed strategy can give reasonable star selection results in all kinds of situations. And based on these star observation instructions, AGRI and GIIRS have implemented more than 35 000 and 35 000 in-orbit star observations, respectively, providing precious data for thermal elastic deformation parameter calculation.

As mentioned above, the moon’s position in the field of view is predicted precisely and automatically. The moon task will be inserted into the time schedule while the moon is forecasted to be suitable for observation. From March 2017 to March 2018, all 194 AGRI moon tasks and 106 GIIRS moon

tasks were arranged automatically through the software of the instrument observation strategies. The details are listed in Tables 14 and 15. A near 100 % success rate validates the effectiveness of the moon forecasts as well as the instrument observation strategies. The occasional unobserved task was because the visible part of the moon was so small that it was invisible in the images.

6 Conclusions

This paper proposed instrument observation strategies specially designed for AGRI and GIIRS on board the FY-4A satellite, the first Chinese three-axis-stabilized geostationary satellite. The requirements of navigation, calibration and earth observation, as well as observation flexibility brought

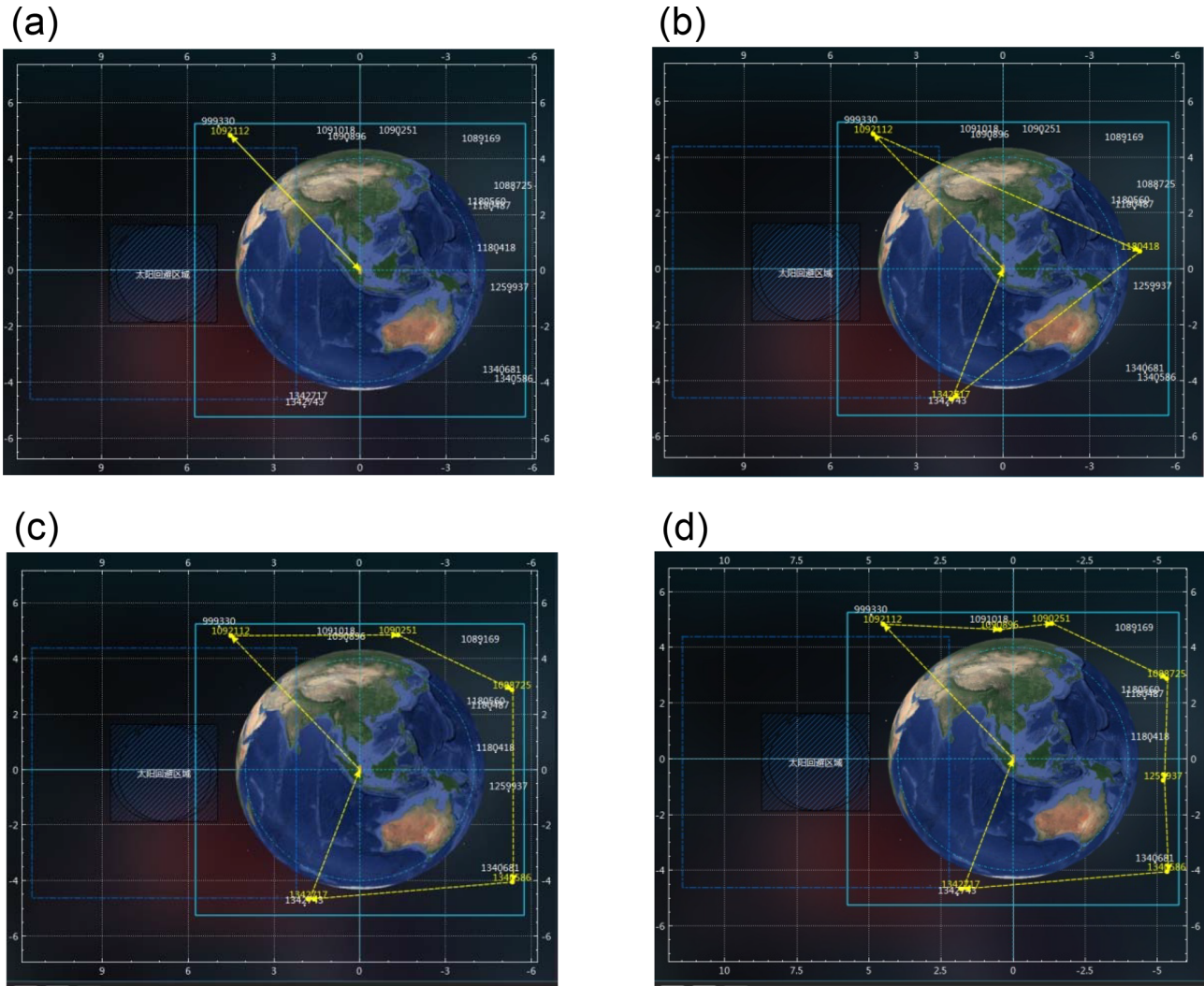


Figure 10. AGRI star selection results – with the sun: (a) the result of choosing one star, (b) the result of choosing three stars, (c) the result of choosing five stars and (d) the result of choosing seven stars.

Table 12. Statistics of AGRI star selection tasks.

No.	Number of stars	Operation success rate	Percentage of all tasks
1	< 3	100 %	0.67 %
2	3	100 %	3.05 %
3	4	100 %	1.53 %
4	5	100 %	94.75 %

Table 13. Statistics of GIIRS star selection tasks.

No.	Number of stars	Operation success rate	Percentage of all tasks
1	< 3	100 %	0.16 %
2	3	100 %	3.42 %
3	4	100 %	0.76 %
4	5	100 %	95.66 %

by the three-axis-stabilized platform, are theoretically considered. The most complicated part, star observation strategies, is proposed to select proper stars to be observed by the instruments, whose information is essential for accurate image navigation. Both simulation results and in-orbit application results are given, including instrument observation strategies, star observation strategies and moon tasks,

showing the validity of the proposed observation strategies. The strategies have been successfully used in FY-4A in-orbit tests for more than a year, helping to accomplish more than 163 000 and 169 000 tasks with AGRI and GIIRS, respectively, laying important foundations for the instruments' daily operation.

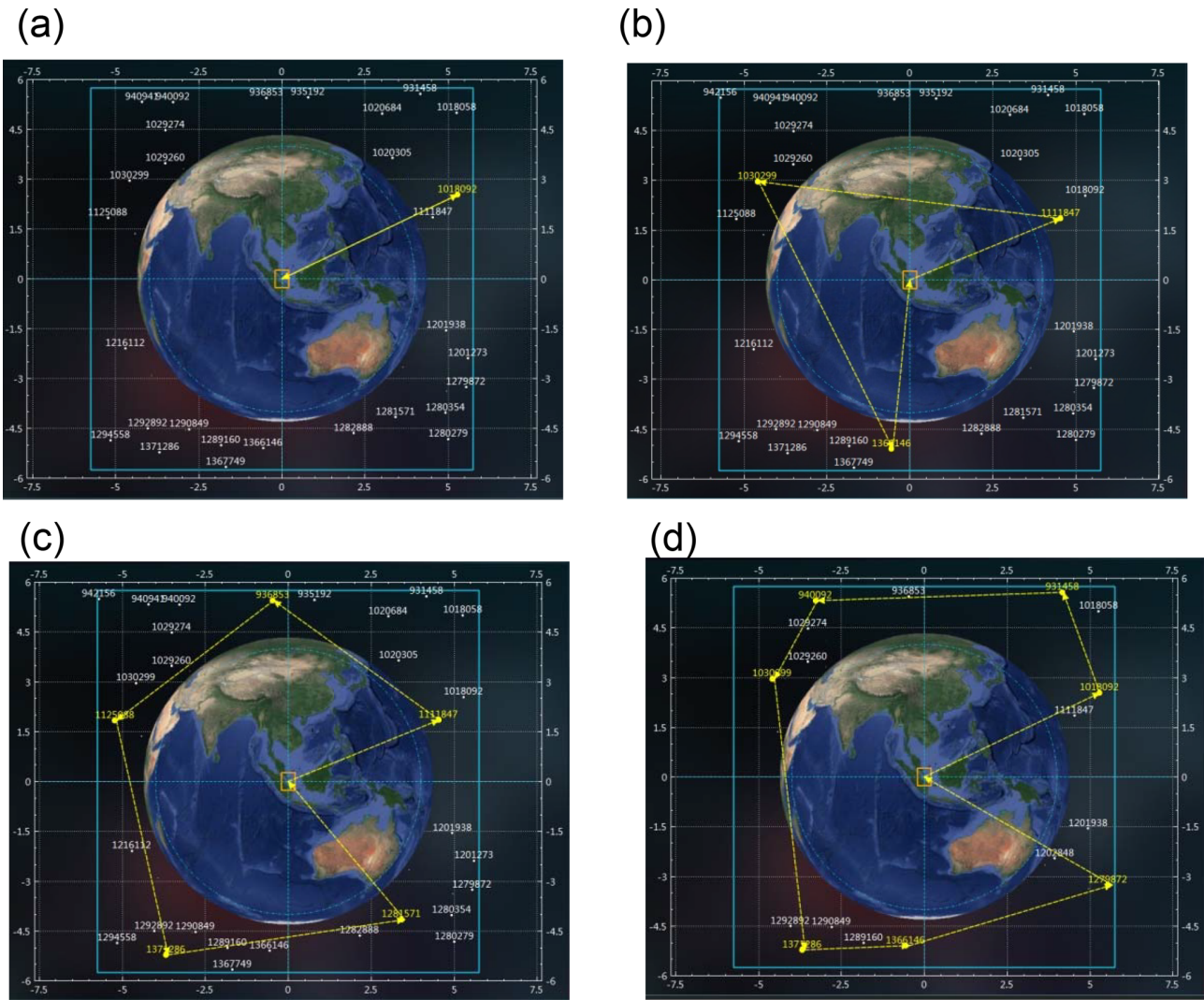


Figure 11. GIIRS star selection results – without the sun: (a) the result of choosing one star, (b) the result of choosing three stars, (c) the result of choosing five stars and (d) the result of choosing seven stars.

Table 14. Statistics of AGRI moon tasks.

Time YYYY-MM	Tasks arranged	Observation success rate
2017-03	12	100 %
2017-04	20	95 %
2017-05	38	100 %
2017-06	16	100 %
2017-07	18	100 %
2017-08	18	100 %
2017-09	7	100 %
2017-10	12	100 %
2017-11	18	100 %
2017-12	19	100 %
2018-01	7	100 %
2018-02	6	100 %
2018-03	3	100 %

Table 15. Statistics of GIIRS moon tasks.

Time YYYY-MM	Tasks arranged	Observation success rate
2017-03	8	100 %
2017-04	0	–
2017-05	2	100 %
2017-06	11	100 %
2017-07	16	100 %
2017-08	16	100 %
2017-09	5	100 %
2017-10	8	100 %
2017-11	7	100 %
2017-12	13	100 %
2018-01	8	100 %
2018-02	6	100 %
2018-03	6	100 %

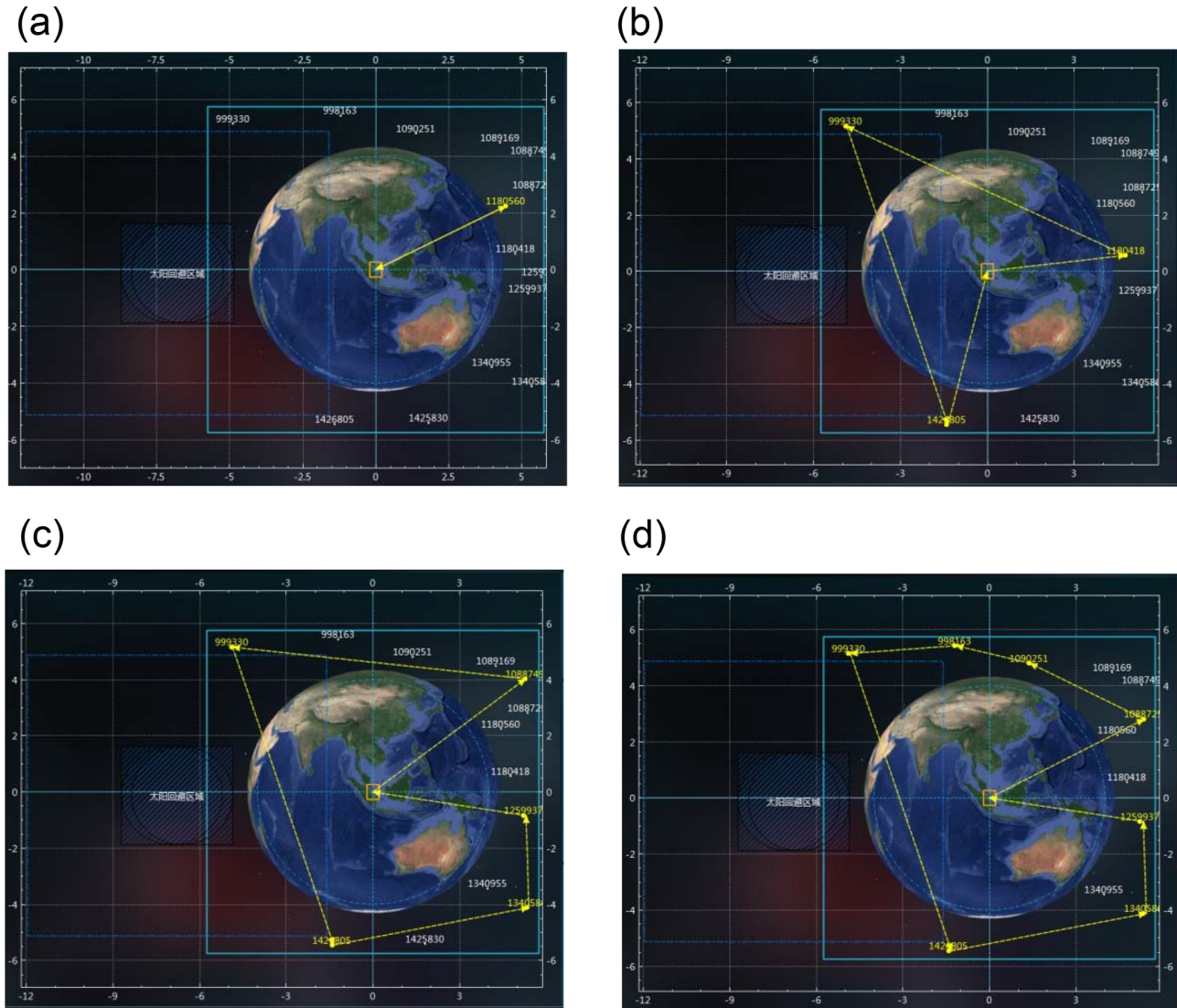


Figure 12. GIIRS star selection results – with the sun: (a) the result of choosing one star, (b) the result of choosing three stars, (c) the result of choosing five stars and (d) the result of choosing seven stars.

So far, the star observation of FY-4A has concentrated on visible stars. With the development of satellites and instruments, star observation using other bands should also be considered in the future. The star observation strategy needs to be specially designed for each observation band according to the band's characteristics. Magnitude limitation, star observation number, angel deviation, etc., should be modified. A whole set of star observation strategies must be proposed for registration of the bands as well as high-precision navigation. And the instrument observation strategy will also be more complicated for the follow-up instruments.

Data availability. The research data can be accessed by direct request to the corresponding author.

Author contributions. JS, LY and ZZ designed the system. PH, HY, SZ and XC developed the software. CL, JW and LZ took part in the discussion. JS and HY processed the data. JS prepared the article with contributions from all co-authors.

Competing interests. The authors declare that they have no conflict of interest.

Acknowledgements. We would like to thank Lei Ding, Ganq Wang and Chang Han from Shanghai Institute of Technical Physics, Chinese Academy of Sciences, for their excellent instrument design and helpful discussions. We are grateful to the entire FY-4 team of the National Satellite Meteorological Center, China Meteorological Administration for durable and in-depth research on the ground sys-

tem of FY-4A satellite. We would also like to thank the reviewers for helping us to improve the paper. This work was supported by the National Natural Science Foundation of China (61172113 and 91338109).

Financial support. This research has been supported by the National Natural Science Foundation of China (grant nos. 61172113 and 91338109).

Review statement. This paper was edited by Jothiram Vivekanandan and reviewed by two anonymous referees.

References

- DOC, NOAA, NESDIS, and NASA: GOES-R series concept of operations (CONOPS), available at: <https://www.goes-r.gov/syseng/docs/CONOPS.pdf> (last access: 16 July 2019), 2016.
- DOC, NOAA, NESDIS, and NASA: Product definition and users' guide (PUG) volume 4: GOES-R rebroadcast (GRB), available at: <https://www.goes-r.gov/users/docs/PUG-GRB-vol4.pdf> (last access: 16 July 2019), 2017.
- Dong, Y.: FY-4 meteorological satellite and its application prospect, *Aerospace Shanghai*, 33, 1–8, 2016.
- Gibbs, B. P., Uetrecht D. S., Carr J. L., and Sayal C.: Analysis of GOES-13 orbit and attitude determination, *Space Ops 2008 Conference of the American Institute of Aeronautics and Astronautics*, 12–16 May 2008, Heidelberg, Germany, <https://doi.org/10.2514/6.2008-3222>, 2008.
- Harris, J. and Just, D.: INR performance simulations for MTG, *Space Ops 2010 Conference of the American Institute of Aeronautics and Astronautics*, 25–30 April 2010, Huntsville, Alabama, USA, <https://doi.org/10.2514/6.2010-2322>, 2010.
- Li, Q. and Dong, Y.: Achievement and forecast of meteorological satellite technology in China, *Aerospace Shanghai*, 25, 1–10, <https://doi.org/10.3969/j.issn.1006-1630.2008.01.001>, 2008.
- Li, X., Wang, G., and Chen, G.: FY-4 imager: visible channel star sensing, *Sci. Technol. Eng.*, 7, 993–996, 2007.
- Lu, F., Zhang, X., and Xu, J.: Image navigation for the FY2 geostationary meteorological satellite, *J. Atmos. Ocean. Tech.*, 25, 1149–1165, <https://doi.org/10.1175/2007JTECHA964.1>, 2008.
- NOAA and NASA: GOES N data book (Rev B), Washington, D.C., USA, 2005.
- Shang, J., Liu, C., Yang, L., Zhang, Z., and Wang, J.: Misalignment angle calculation accuracy analysis of three-axis stabilized geostationary satellite, *J. Geosci. Env. Prot.*, 5, 153–165, 2017.
- Shang, J., Zhang, Z., Liu, C., and Yang, L.: Observation mode and region segmentation of new generation geostationary meteorological satellite of China, *Meteor. Env. Res.*, 9, 1–4, 2018.
- Yang, L. and Shang, J.: Modeling and computation on the attitude misalignment parameters for geostationary meteorological satellite, *Chinese J. Electron.*, 20, 370–374, <https://doi.org/10.3969/j.issn.0372-2112.2011>.
- Zhang, H., Su, Y., Shang, J., Yang, L., Cai, B., Liu, C., Wang, J., Zhou, S., and Zhang, Z.: Accurate star centroid detection for the Advanced Geosynchronous Radiation Imager of Fengyun-4A, *IEEE ACCESS*, 6, 7987–7999, <https://doi.org/10.1109/ACCESS.2018.2798625>, 2018.
- Zhang, Z., Dong, Y., Ding, L., Wang, G., Fang, X., Zhang, X., and Huang, F.: China's first second-generation FY-4 meteorological satellite launched, *Space Int.*, 12, 6–12, 2016.